Anodic oxidation of gallium nitride

A. PAKES, P. SKELDON, G. E. THOMPSON
Corrosion and Protection Centre, University of Manchester Institute of Science and Technology, P.O. Box 88, Manchester, M60 1QD, UK
E-mail: p.skeldon@umist.ac.uk

J. W. FRASER, S. MOISA, G. I. SPROULE, M. J. GRAHAM
Institute for Microstructural Sciences, National Research Council of Canada, Montreal Road, Ottawa, KIA OR6, Canada

S. B. NEWCOMB
Materials and Surface Science Institute, University of Limerick, Limerick, Republic of Ireland

The anodic oxidation of n-type GaN (carrier concentration 4.6×10^{18} cm^{-3}) under laboratory illumination at a constant current density of 5 mA cm^{-2} in sodium tungstate electrolyte is examined by high resolution microscopy and surface analysis. The GaN, deposited as a thin layer by molecular beam epitaxy, had an initially faceted surface. Anodic oxidation gives rise to local growth of an amorphous Ga_2O_3-based reaction product, often, but not exclusively, located in the vicinity of troughs formed by intersecting facets. At these regions dislocations in the GaN intersect the surface. The product is non-uniform in thickness and morphology, with pore-like features. With prolonged anodic treatment, local oxidation progresses as channels, which eventually reach the base of the GaN layer, leaving a porous skeleton. The formation of a uniform and compact film material on GaN is considered to be impeded by generation of nitrogen from the anodic reaction, with the strength of the Ga–N bonding focusing oxidation on regions of increased impurity, non-stoichiometry or defect concentration. © *2003 Kluwer Academic Publishers*

1. Introduction

GaN is of interest for electronic and optoelectronic devices. In order to develop such applications, understanding of the electrochemical response for pretreatment and processing is necessary. Minsky *et al.* [1] reported that etching, without applied current, of n-type GaN, with a carrier concentration (cc) of 2–4 × 10^{17} cm^{-3}, in KOH and HCl solutions required laser illumination. Yoshida *et al.* [2] found that n-type GaN (cc 1.3×10^{19} cm^{-3}) was etched by anodic treatment in KOH solution, with UV illumination increasing the etching rate. Application of voltage was essential for etching of high quality GaN, but not for lower quality material. The presence of oxygen in NaOH solution reduced the potentiostatic etching in the dark of n-type GaN (cc 4×10^{18} cm^{-3}) [3].

Lu *et al.* reported that etching at constant current of n-type GaN (cc 5×10^{17} cm^{-3}) in tartaric acid/ethylene glycol solution required UV illumination [4]. Without illumination, deep cavities developed that were related to the presence of dislocations and non-stoichometric regions in the GaN. Yamamoto *et al.* [5] observed that, regardless of illumination, the voltage remained low during the early stages of anodic oxidation of GaN in NaOH and H_2SO_4 solutions at constant current, suggesting selective dissolution of regions of low quality and/or high carrier concentration. Rotter *et al.* [6] demonstrated that under potentiostatic conditions, with UV illumination, oxide films of about 0.4 μm thickness formed in KOH solution.

Youtsey *et al.* [7] produced smooth n-type GaN surfaces using photoelectrochemical etching in unstirred KOH solution under a mercury-arc lamp. Without illumination, no etching resulted. At low and high intensities of illumination, the etching rate depended upon generation of electron-hole pairs and diffusion of electrolyte species to the semiconductor surface where reaction proceeded. Under specific conditions, preferential etching of material between dislocations produced nanometre-sized whiskers of GaN in KOH solution [8].

The previous studies of the etching behaviour indicate the importance of the carrier concentration and illumination on the response, with the possibility of non-uniform attack under certain conditions. The present paper reports the anodic behaviour of GaN in sodium tungstate electrolyte, which supports anodic film growth at high efficiency on other gallium-containing III–V semiconductors, such as GaAs and GaP [9, 10]. Here, the particular interest is the nature of reaction products developed, and the detailed morphology of the treated surface, which were investigated by atomic force (AFM), scanning electron (SEM) and transmission electron microscopies (TEM), with

0022–2461 © *2003 Kluwer Academic Publishers*

chemical analysis by X-ray photoelectron (XPS) and Auger electron spectroscopies (AES).

2. Experimental

n-type GaN (cc 4.6×10^{18} cm^{-3}), of thickness 1.7 μm, was deposited by molecular beam epitaxy onto a sapphire substrate. After rinsing in acetone, specimens were anodically oxidized, under normal laboratory illumination, at 5 mA cm^{-2} in 0.1 M $Na_2WO_4 \cdot 2H_2O$ at 298 K, and then dried in a nitrogen stream.

Plan view examinations, prior to and following anodic treatment, were accomplished using a Digital Instruments Nanoscope III AFM in the tapping mode. An Hitachi S-4700 FEGSEM was utilised for observation of plan-views and cross-sections, with the latter produced by cleaving the specimen normal to the macroscopic surface. XPS and AES analyses were carried out respectively in a PHI 5500 system, with a monochromated Al K_α source, and AES in a PHI 650 system.

Sections for transmission electron microscopy were produced using focused ion beam (FIB) thinning procedures; small rectangular bars, of dimensions $2.8 \times 1.0 \times 0.05$ mm were mounted on Cu support grids, and ion milling was carried out at 30 kV. Samples were examined in a JEOL 2000FX instrument.

3. Results

3.1. Surface prior to anodic treatment

An AFM image of the GaN following rinsing in acetone reveals a serrated surface formed by intersecting facets, with a peak-to-peak distance between 100 and 500 nm (Fig. 1). The peak-to-trough distance varies between 15 nm and 200 nm, with an average value of approximately 80 nm. SEM images confirm the faceting, with peaks appearing as light regions in a cellular arrangement (Fig. 2). A bright field transmission electron micrograph of the GaN discloses a defective microstructure, with a high density of defects particularly within about 500 nm of the sapphire/GaN interface (Fig. 3a). Strain is evident in the sapphire, as indicated by the contrast marked at A. The peak-to-peak and peak-to-trough distances are between 150 and 300 nm and 60 to 80 nm respectively in the area sampled by the section (Fig. 3b) in reasonable agreement with AFM and SEM images. Examination of several sections indicates that dislocations are associated largely with troughs in the as-grown material (Fig. 3b).

3.2. Voltage-time behaviour

The typical voltage–time behaviour for anodic oxidation of GaN (Fig. 4) shows an approximately linear slope of 3.3 V s^{-1} from the commencement of anodizing to about 12 V. Subsequently the slope decreases to approximately 0.7 V s^{-1}, which is maintained from about 3.5 s until anodizing was terminated at approximately 28 V. A further specimen was anodized for a protracted time; in this case the voltage again achieved approximately 28 V and then increased as the oxidation front reached the sapphire substrate. At this stage the charge passed was 2.2 C cm^{-2}; the resultant specimen was examined by SEM only.

3.3. Surface following anodic treatment

An AFM image of GaN following anodic oxidation to 28 V shows a nodular appearance (Fig. 5) in contrast to the initial faceted surface. The peak-to-trough distance is between 10 and 100 nm, less than that prior to anodic oxidation. The distance between nodules is between 20 and 300 nm, similar to the peak-to-peak distances of the original surface. The surface also reveals a height modulation over greater distances than the spacing of adjacent nodules.

A scanning electron micrograph of the cross-section of anodically-treated GaN discloses rounded regions of localized oxidation separated by protrusions of relatively unattacked material, (positions A, Fig. 6a). The local attack appeared to proceed preferentially in the vicinity of troughs in the initial surface. The depth of attack ranges from 60 to 200 nm. The material of dark appearance, at position C, is due to the influence of surface regions behind the plane of the cross-section. An isolated region of attack, at position B, is probably connected to the surface via a channel of preferential oxidation outside the section. The specimen subjected to prolonged anodic treatment revealed a skeletal morphology with columns or plates of apparently

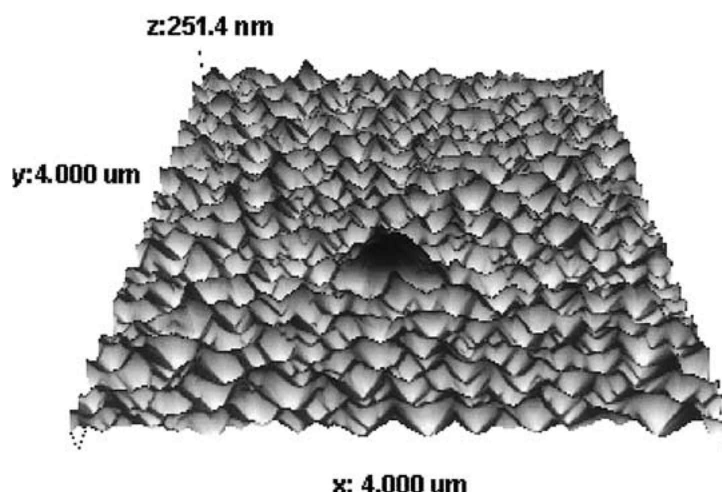

Figure 1 AFM image of the surface of GaN after rinsing in acetone.

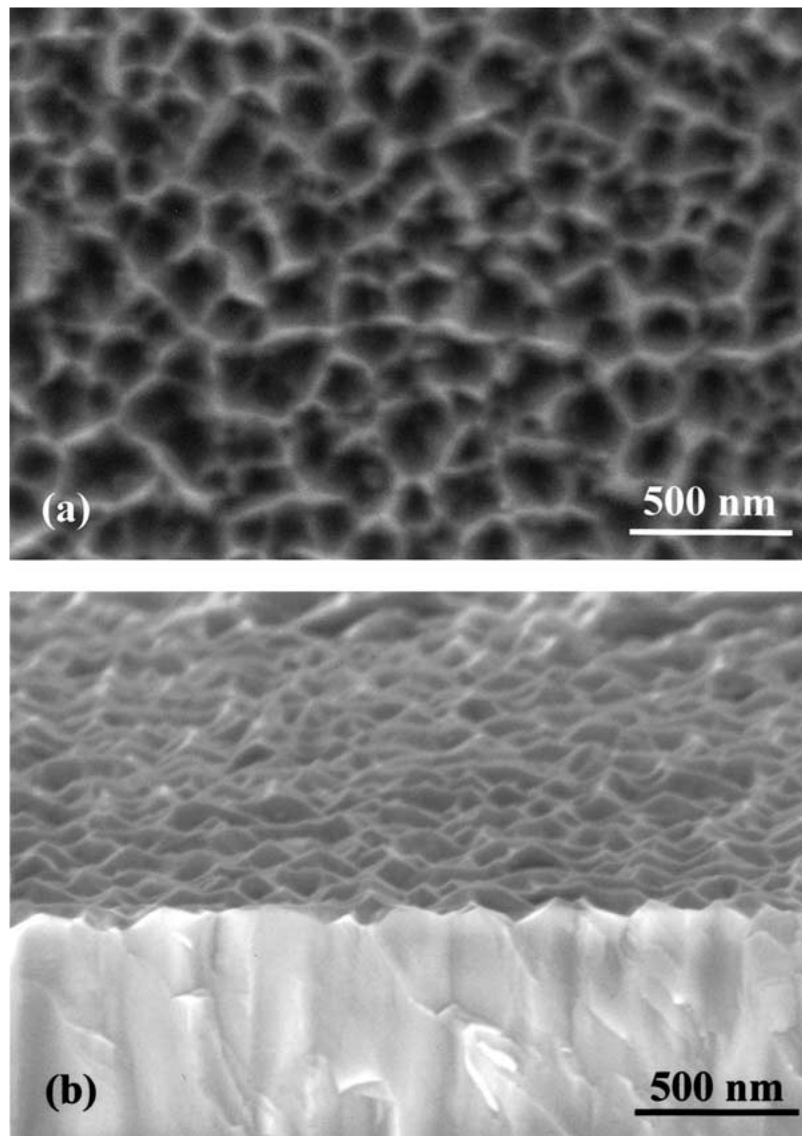

Figure 2 Scanning electron micrographs of GaN following rinsing in acetone: (a) plan view; (b) cleaved cross-section.

unattacked material and intervening regions of porosity and/or oxidation product extending as channels through the GaN layer (Fig. 6b).

Transmission electron micrographs confirm the formation of regions where local oxidiation of the GaN has taken place, separated by protrusions that are remnants of the faceted surface (position A, Fig. 7a). Material at regions of local oxidation, (positions B and C), identified as amorphous by electron diffraction, is reaction product that is generally found in the vicinity of troughs, although there is also some lateral spread. The material (which was not evident by SEM) is of non-uniform appearance and contains pore-like features, which are generally less than 10 nm diameter. The extent of local oxidation ranges from 90 to 180 nm, similar to that revealed by SEM. Areas of attack under the GaN surface (position D, Fig. 7b) are considered to result from the lateral spread of attack outside the plane of the section.

AES was undertaken to gain further insight into the nature of the reaction product. The AES profile for anodically oxidized GaN reveals the presence of oxygen, gallium associated with oxygen, and tungsten, suggesting the reaction product is gallium oxide, with some incorporated tungsten species (Fig. 8). The roughness and non-uniformity of the substrate/oxide interface result in broadening of the profiles, as expected. The XPS survey spectrum discloses the presence of Ga, W and N, and C contaminant. High resolution scans (referenced to the C 1s line of 284.8 eV) for Ga 3d (B.E = 20.6 eV) and Ga 2p (B.E = 1118.9) peaks indicate the presence of Ga_2O_3. Scrutiny of the O 1s peak indicates negligible contribution from hydroxide. The W 4d and W 4f peaks suggest either WO_3 or WO_4^{2-}. The N 1s peak is in the same region as a strong contribution from the Ga LMM1 Auger peak. Nevertheless, deconvolution of the peak indicates a signal from N in the GaN substrate.

4. Discussion

From previous work on GaN, it is clear that etching is affected significantly by the carrier concentration, illumination, the distribution of impurities and non-stoichiometry, and defects [1, 7]. GaN of low carrier concentration is difficult to etch in the absence of illumination, probably due to the strength of the Ga—N bond [5]. Further, etching of GaN can proceed preferentially, leading to cavities or channels, due to attack of more readily oxidized regions of material. In

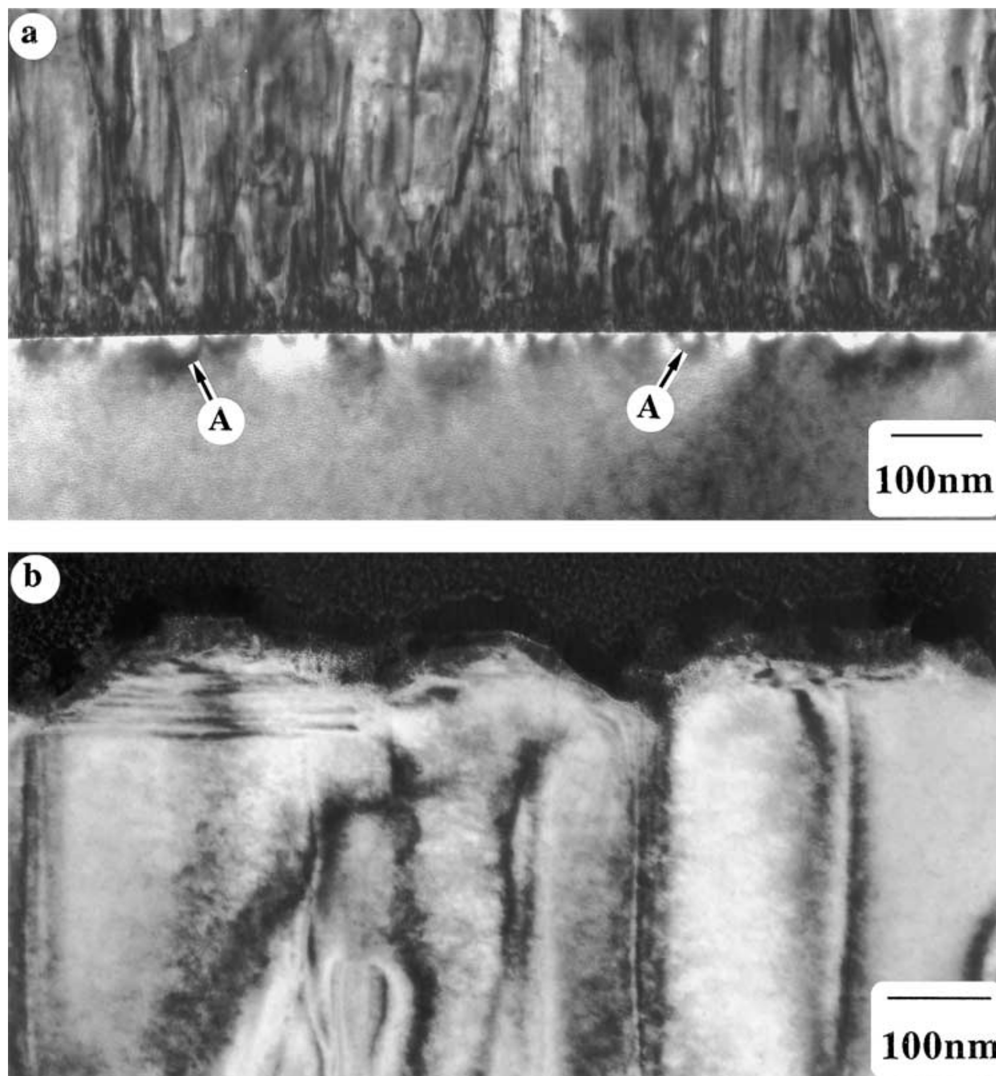

Figure 3 Bright field transmission electron micrographs of cross-sections of GaN after rinsing in acetone: (a) the sapphire/GaN interface; (b) the faceted GaN appearance.

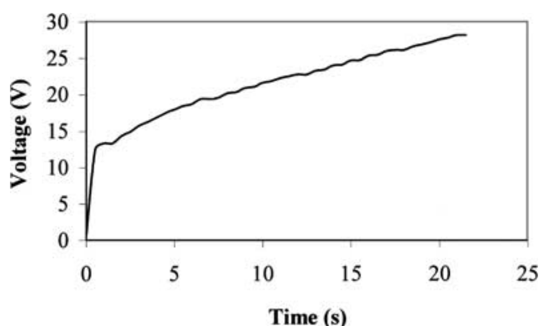

Figure 4 Voltage-time response during anodic oxidation of GaN at 5 mA cm^{-2} in 0.1 M sodium tungstate electrolyte at 298 K.

the present experiments, using conditions conducive to anodic oxide formation, such local oxidation was observed, with adjacent regions appearing to be little changed. The preservation of the latter regions can be attributed to the greater purity/perfection of the GaN, and the lack of UV irradiation to assist oxidation. Elsewhere, anodic oxidation proceeded comparatively readily, with the local current density differing from the average value due to local anodic oxidation and roughening of the surface. The local oxidation occurred particularly, but not exclusively, in the regions of troughs in the faceted initial surface and may be associated with dislocations emerging at these sites.

The oxidation product differed significantly from a compact, amorphous anodic film. TEM revealed a textured appearance, including pore-like features generally of less than 10 nm diameter, with XPS suggesting the generation of Ga_2O_3. The product differs from amorphous Ga_2O_3 formed by anodizing of GaP in sodium tungstate electrolyte, which develops as a uniform, non-porous layer above an inner layer containing both Ga and P species [9]. The film on GaP grows by high field ionic conduction with the faster migration of gallium species relative to phosphorus species leading to the outer layer of Ga_2O_3.

The absence of a compact film material in the oxidised regions of the GaN substrate may be due to generation of N_2 gas during anodic oxidation, which has been suggested to proceed according to the reaction [11].

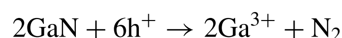

$$2\text{GaN} + 6\text{h}^{+} \rightarrow 2\text{Ga}^{3+} + \text{N}_2$$

The nitrogen, generated at the GaN/oxide interface, may be partly trapped within the Ga_2O_3, hence producing non-uniform material. Amorphous anodic films,

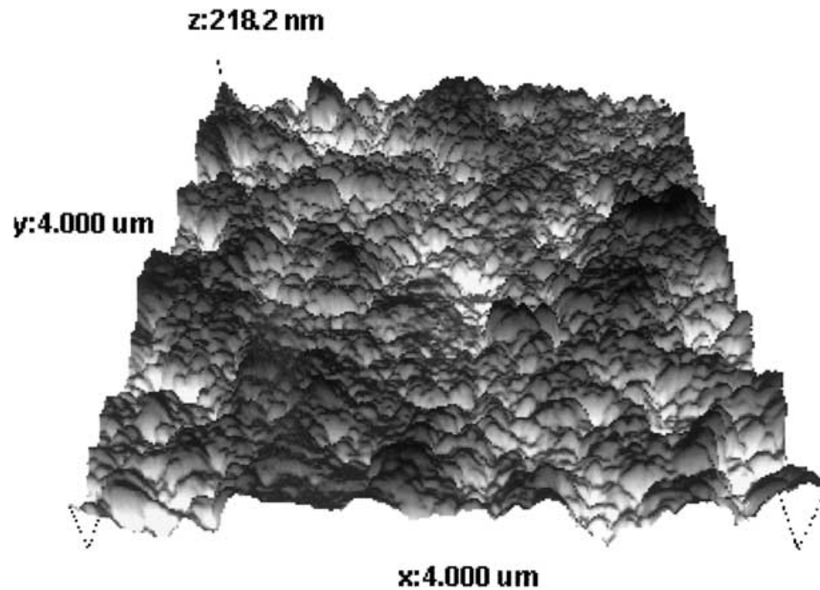

Figure 5 AFM image of GaN following anodic oxidation at 5 mA cm^{-2} in 0.1 M sodium tungstate electrolyte at 298 K.

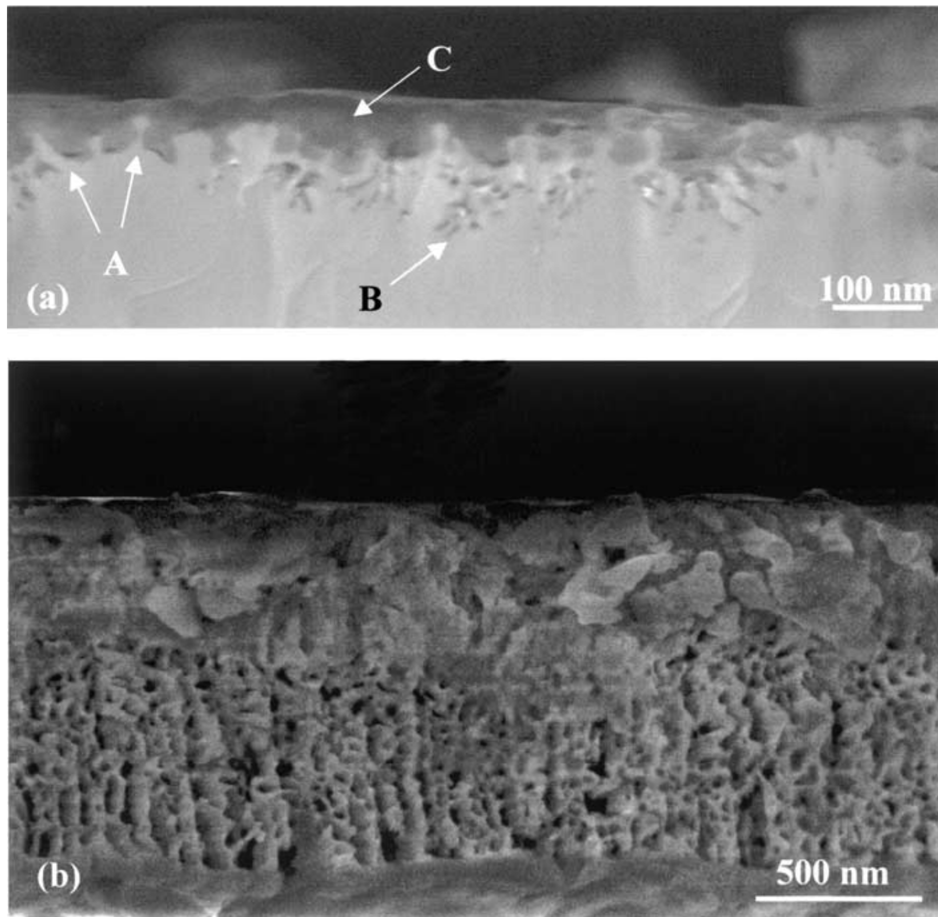

Figure 6 Scanning electron micrographs of cleaved GaN after anodic oxidation at 5 mA cm^{-2} in 0.1 M sodium tungstate at 298 K: (a) anodised to 28 V; (b) anodised for a prolonged period.

such as those formed on dilute Al-Cu alloys, have a remarkable capacity for accommodating high pressure gas bubbles, formed within the film close to the substrate/film interface, which can expand and coalesce to a significant degree without cracking of the growing oxide [12]. The film material and trapped gas support the voltage that develops during anodizing. For Al-Cu alloys, oxygen is generated from O^{2-} ions of the Al_2O_3 at sites of semiconducting oxide associated with oxidation of Cu in the alloy. For alloys of high copper contents, the resultant anodic film is extensively flawed and the voltage rise due to normal film growth is limited to a low value. In the case of GaN, the film material is also presumably highly flawed and fragile due to the large amounts of nitrogen generated, in this case due to oxidation of the substrate which, consequently, impede growth of uniform Ga_2O_3. The absence of formation of nitrogen compounds contrasts with oxidation of P and

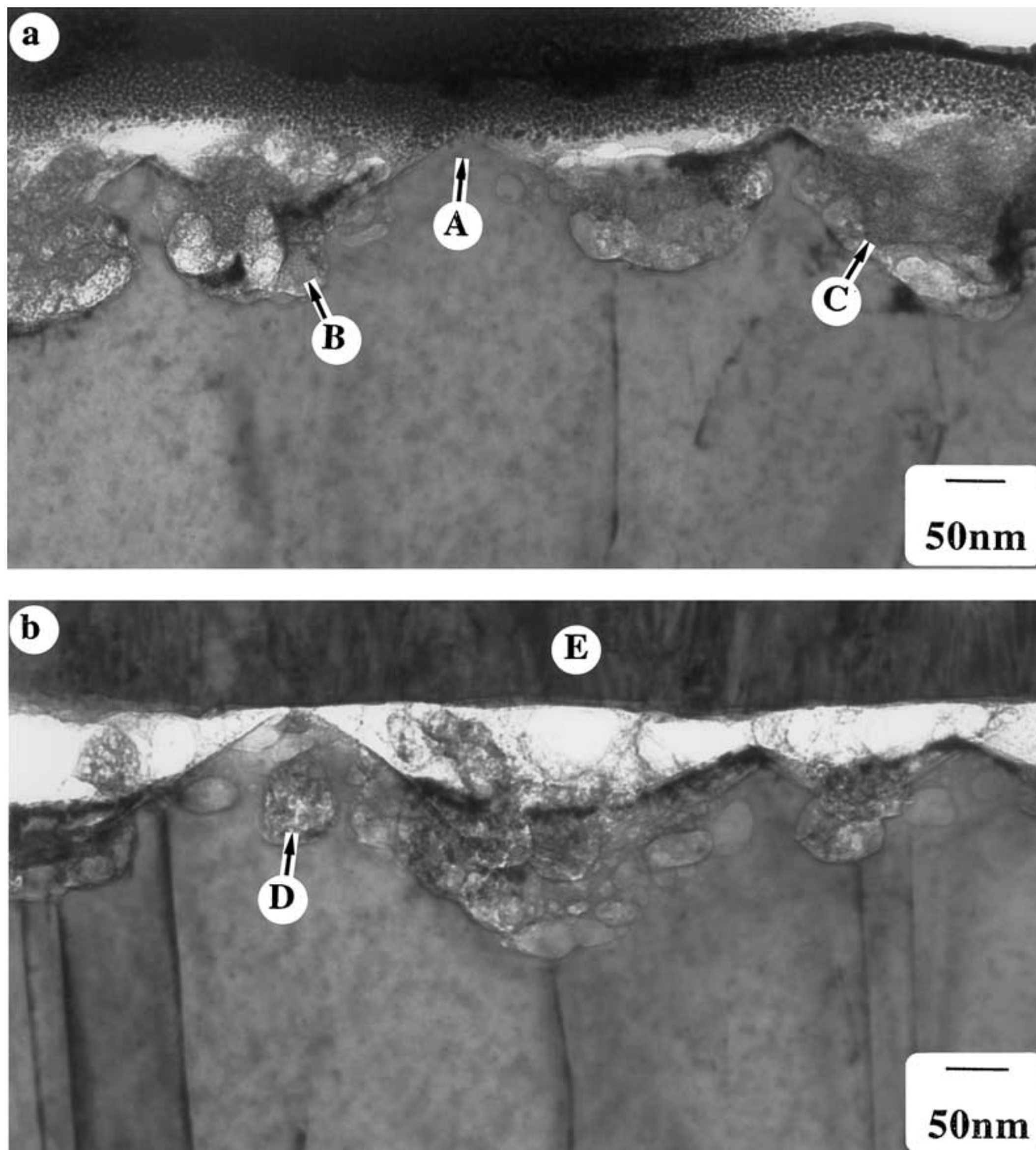

Figure 7 Bright field transmission electron micrographs of cross-sections of GaN after anodic oxidation to 28 V at 5 mA cm^{-2} in 0.1 M sodium tungstate electrolyte at 298 K (a, b). Region E in (b) is a mask used in the TEM sample preparation.

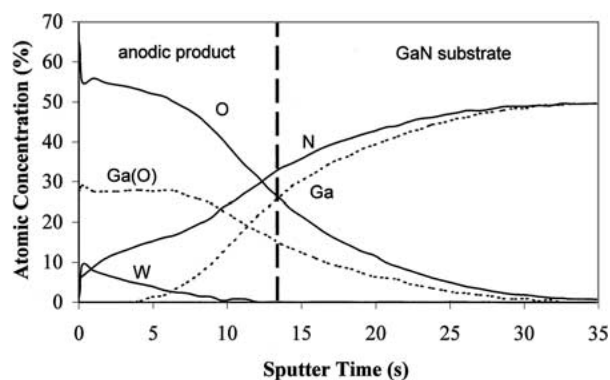

Figure 8 Auger electron spectroscopy profile of GaN anodized at 5 mA cm^{-2} to 28 V in 0.1 M sodium tungstate at 298 K. Sputtering used 1 keV argon ions.

As and formation of film species (e.g. P_2O_5, As_2O_3) during anodising of GaP and GaAs [9, 10]. Tungsten species associated with reaction product, probably arise from adsorbed W ions, WO_3, formed by reaction of electrolyte anions with the H^+ ion by-product of the anodic reaction, or tungsten species incorporated into the Ga_2O_3 [13]. The reported formation of uniform films of 0.4 μm thickness in KOH [6] at relatively low voltage suggests that the film material did not develop by a high-field process.

The anodic oxidation of the present GaN is concentrated in regions of troughs of the faceted GaN. However, the attack is not exclusive to these regions, as is evident from cavity-like features in the regions of peaks. Further, adjacent to such features are flat surfaces, where the loss of material due to anodic oxidation is negligible. The localized nature of the anodic oxidation suggests non-uniformity of the substrate, with oxidation occurring at regions of enhanced impurity, greater non-stoichiometry, or higher defect concentration which, in particular, may be associated with regions at and adjacent to dislocations.

Localization of the anodic process was emphasized by prolonged oxidation of the GaN until the oxidation front reached the sapphire substrate. Using a density of 6.1×10^3 kg m^{-3} for GaN [11], the charge passed was then equivalent to a depth of uniform oxidation of 1.0 μm, compared with the initial thickness of GaN of

1.7 μm. This indicates that the material regions that readily oxidized comprised about 61% of the volume of GaN. Such an estimate is reasonably consistent with the channel-like porous morphology observed by SEM. Additional high resolution studies are required to understand filming of GaN in more detail, focusing on the film morphology and detection of nitrogen gas within bubbles.

5. Conclusions

1. Anodic oxidation of GaN, of carrier concentration 4.6×10^{18} cm^{-3}, under normal laboratory illumination, at 5 mA cm^{-2} in 0.1 M sodium tungstate electrolyte at 293 K results in local oxidation attack of the substrate. The oxidation occurs preferentially at troughs in the faceted GaN substrate, although oxidation also takes place at other regions. At certain regions, particularly associated with peaks in the faceted substrate, oxidation is negligible. The localized nature of the oxidation of the GaN is presumed to be related to the strength of the Ga—N bond and non-uniform distributions of impurity, non-stoichiometry or defects in the substrate.

2. At regions of anodic oxidation, Ga_2O_3 is formed. The product has a non-uniform, textured appearance with pore-like features. The absence of a compact anodic film is probably due to extensive generation of nitrogen during anodic oxidation which disrupts development of a uniform anodic film.

Acknowledgements

The authors acknowledge financial support from the Joint Science and Technology Fund of the National Research Council of Canada and the British Council; they also thank Dr J. Webb for supplying the GaN.

References

1. M. S. MINSKY, M. WHITE and E. L. HU, *Appl. Phys. Lett.* **68** (1996) 68.
2. S. YOSHIDA, *J. Cryst. Growth* **181** (1997) 293.
3. M. OHKUBO, *Jpn J. Appl. Phys.* **36** (1997) L955.
4. H. LU, Z. WU and I. BHAT, *J. Electrochem. Soc.* **144** (1997) L8.
5. A. YAMAMOTO, Y. TSUJI, T. SUGIURA and A. HASHIMOTO, *Jpn J. Appl. Phys.* **38** (1996) 2619.
6. T. ROTTER, D. MISTELE, J. STEMMER, F. FELDER, J. ADERHOLD, P. GAUL, V. SCHEWGLER, C. KIRCHNER, M. KAMP and M. HEUKEN, *Appl. Phys. Lett.* **76** (2000) 3923.
7. C. YOUTSEY, I. ADESIDA, L. T. ROMANO and G. BULMAN, *ibid.* **72** (1998) 560.
8. C. YOUTSEY, L. T. ROMANO and I. ADESIDA, *ibid.* **73** (1998) 797.
9. F. ECHEVERRIA, P. SKELDON, G. E. THOMPSON, G. C. WOOD, H. HABAZAKI and K. SHIMIZU, *J. Electrochem. Soc.* **145** (1998) 3011.
10. H. HABAZAKI, P. SKELDON, D. GHIDAOUI, S. B. LYON, K. SHIMIZU, G. E. THOMPSON and G. C. WOOD, *J. Phys. D: Appl. Phys.* **29** (1996) 2545.
11. C. YOUTSEY, I. ADESIDA and G. BULMAN, *Appl. Phys. Lett.* **71** (1997) 2151.
12. P. SKELDON, G. E. THOMPSON, X. ZHOU, H. HABAZAKI and K. SHIMIZU, *Phil. Mag.* A **76** (1997) 729.
13. G. C. WOOD, P. SKELDON, G. E. THOMPSON and K. SHIMIZU, *J. Electrochem. Soc.* **143** (1996) 74.

Received 16 July 2001
and accepted 24 September 2002